Wnt/β-catenin signaling controls development of the blood–brain barrier

Stefan Liebner,[1] Monica Corada,[3] Thorsten Bangsow,[2] Jane Babbage,[4] Andrea Taddei,[3] Cathrin J. Czupalla,[1] Marco Reis,[1] Angelina Felici,[3] Hartwig Wolburg,[5] Marcus Fruttiger,[6] Makoto M. Taketo,[7] Harald von Melchner,[2] Karl Heinz Plate,[1] Holger Gerhardt,[4] and Elisabetta Dejana[3,8]

[1]Institute of Neurology (Edinger Institute) and [2]Institute of Molecular Hematology, Johann Wolfgang Goethe University, 60325 Frankfurt, Germany
[3]Italian Foundation for Cancer Research Institute of Molecular Oncology, 20139 Milan, Italy
[4]Vascular Biology Laboratory, Cancer Research UK, London Research Institute, London WC2A 3PX, England, UK
[5]Institute of Pathology, Eberhard Karls University, 72076 Tübingen, Germany
[6]Institute of Ophthalmology, University College London, London WC1E 6BT, England, UK
[7]Department of Pharmacology, Graduate School of Medicine, Kyoto University, Sakyo, Kyoto 606-8501, Japan
[8]Department of Biomolecular Sciences and Biotechnologies, School of Sciences, University of Milan, 20126 Milan, Italy

The blood–brain barrier (BBB) is confined to the endothelium of brain capillaries and is indispensable for fluid homeostasis and neuronal function. In this study, we show that endothelial Wnt/β-catenin (β-cat) signaling regulates induction and maintenance of BBB characteristics during embryonic and postnatal development. Endothelial specific stabilization of β-cat in vivo enhances barrier maturation, whereas inactivation of β-cat causes significant down-regulation of claudin3 (Cldn3), up-regulation of plamalemma vesicle-associated protein, and BBB breakdown. Stabilization of β-cat in primary brain endothelial cells (ECs) in vitro by N-terminal truncation or Wnt3a treatment increases Cldn3 expression, BBB-type tight junction formation, and a BBB characteristic gene signature. Loss of β-cat or inhibition of its signaling abrogates this effect. Furthermore, stabilization of β-cat also increased Cldn3 and barrier properties in nonbrain-derived ECs. These findings may open new therapeutic avenues to modulate endothelial barrier function and to limit the devastating effects of BBB breakdown.

Introduction

Endothelial cells (ECs) of brain capillaries form an active permeability barrier and transport system known as the blood–brain barrier (BBB), which is instrumental in the control of the brain fluid milieu (Engelhardt, 2003). Complex tight junctions (TJs) between brain ECs constituted by proteins of the claudin (Cldn) family and occludin (Ocln) seal off the paracellular pathway (Furuse and Tsukita, 2006). Whereas Cldn5 is also found in nonbarrier endothelium, Cldn3 is predominantly present in brain ECs, where it plays a specific role in the establishment and maintenance of BBB TJ morphology (Wolburg et al., 2003; Nitta et al., 2003).

Correspondence to S. Liebner: stefan.liebner@kgu.de; H. Gerhardt: holger.gerhardt@cancer.org.uk; or E. Dejana: elisabetta.dejana@ifom-ieo-campus.it

Abbreviations used in this paper: 4OHT, 4-hydroxy-tamoxifen; BAT-Gal, β-cat–activated transgene driving expression of nuclear β-galactosidase reporter; BBB, blood–brain barrier; β-cat, β-catenin; Cldn, claudin; CM, conditioned medium; EC, endothelial cell; GOF, gain of function; IF, immunofluorescence; IHC, immunohistochemistry; Lef, lymphoid enhancer factor; LOF, loss of function; MBE, mouse brain microvascular EC; Ocln, occludin; P-face, protoplasmic fracture face; Plako, plakoglobin; Plvap, plamalemma vesicle-associated protein; TAT, transactivating regulatory protein; TCF, T cell factor; TJ, tight junction; VE-cad, vascular endothelial cadherin; ZO-1, zonula occludens 1.

The online version of this article contains supplemental material.

BBB ECs also express specific transporters for glucose, amino acids, and, to prevent damage to the brain, members of the multidrug resistance transporter family (also known as ABC transporters; Engelhardt, 2003). ECs rapidly lose their barrier and selective transport properties under pathological conditions in vivo (ischemia and tumor) and upon cultivation in vitro, indicating that the healthy brain provides inductive and maintenance signals for the BBB. Our limited knowledge of the nature of these signals and of the molecular regulation of the BBB hampers the development of BBB model systems and patient therapy (Liebner et al., 2000b; Engelhardt, 2006).

A major pathway regulating brain development is the canonical Wnt/wingless pathway acting via β-catenin (β-cat) stabilization. This favors translocation of β-cat to the nucleus, where it binds to transcription factors of the lymphoid enhancer factor (Lef)/T cell factor (TCF) family, and thus modulates gene

The Rockefeller University Press $30.00
J. Cell Biol. Vol. 183 No. 3 409–417
www.jcb.org/cgi/doi/10.1083/jcb.200806024

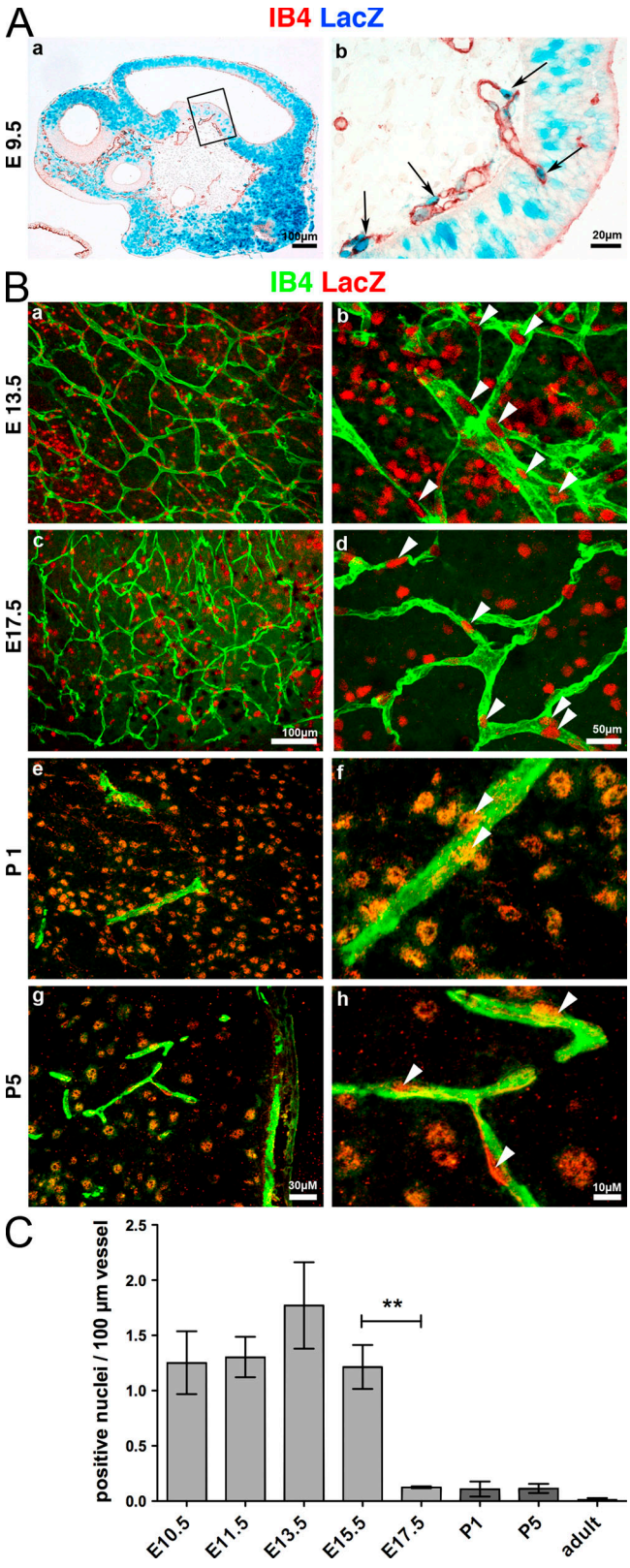

Figure 1. **Canonical Wnt signaling is active in ECs during brain angiogenesis and becomes progressively down-regulated during vessel maturation.** (A) LacZ whole-mount stained (blue) E9.5 BAT-Gal embryos sectioned and counterstained for isolectin B4 (IB4; red). Panel b is a higher magnification of the boxed area in panel a. Arrows point to nuclear LacZ reporter gene staining. (B, a–d) Whole-mount hindbrain staining for LacZ (reflection; red) and IB4 (green) of BAT-Gal embryos (E13.5 and 17.5) analyzed by confocal microscopy. Arrowheads indicate LacZ-positive nuclei. (B, e–h) Staining of brain cryosections from postnatal BAT-Gal pups (P1 and P5) for LacZ (immunofluorescence [IF], red) and IB4 (green). Arrowheads indicate LacZ-positive nuclei. Positive nuclei outside the vascular system indicate active Wnt signaling in the brain parenchyma. (C) Quantification of LacZ-positive nuclei per 100-μm vessel length shows a significant decrease from E15.5 to 17.5 (five fields per hindbrain; three brains; **, P = 0.0003). Error bars represent SEM.

transcription (Moon, 2005). In this study, we report that Wnt/β-cat signaling in brain ECs in vitro and in vivo during brain angiogenesis and postnatal vascular maturation is necessary to induce barrier properties in brain ECs.

Results and discussion

Active endothelial β-cat signaling correlates with central nervous system vascularization, BBB development, and maturation

In β-cat–activated transgene driving expression of nuclear β-galactosidase reporter (BAT-Gal) mice for Wnt/β-cat signaling, we observed strong LacZ-reporter activity in ECs starting at embryonic day (E) 9.5 when the perineural vascular plexus is fully developed (Fig. 1 A, a and b). Throughout brain angiogenesis up to E15.5, numerous ECs in the immature network were LacZ positive (Fig. 1 B, a and b). From E15.5 to 17.5, the number of LacZ-positive nuclei decreased significantly (Fig. 1, B [c and d] and C) to a level that was maintained during early postnatal stages in vessels of the cortex (Fig. 1, B [e–h] and C). Adult brain vessels rarely displayed LacZ-positive nuclei, suggesting that Wnt signaling activity is required for BBB maturation but is low when the BBB is fully mature (Fig. 1 C and not depicted).

Conditional activation or inactivation of endothelial β-cat in vivo modulates Cldn3 and plamalemma vesicle-associated protein (Plvap) expression and BBB permeability

To understand the role of β-cat in BBB maturation and maintenance, we selectively deleted β-cat in ECs (loss of function [LOF]) at postnatal day (P) 4, P7, and P14, corresponding to stages of progressive BBB maturation (Kniesel et al., 1996). For this purpose, we crossed $\beta cat^{lox/lox}$ mice with tamoxifen-inducible Pdgfb-iCreERT2 mice (Brault et al., 2001; Claxton et al., 2008). Cre expression was monitored by EGFP expression (the Pdgfb-iCreERT2 allele includes an internal ribosome entry-EGFP sequence), and recombination was tracked by crossbreeding with ROSA26R::YFP Cre reporter mice (Srinivas et al., 2001; unpublished data). After induction of Cre-mediated recombination by 4-hydroxy-tamoxifen (4OHT) in $\beta cat^{lox/lox}$/Pdgfb-iCreERT2 mice, immunolabeling for β-cat demonstrated complete absence of the protein in nearly all brain vessels at P4 (Fig. S1, available at http://www.jcb.org/cgi/content/full/jcb.200806024/DC1) and P7 and in ∼50% at P14 (not depicted). In Cre^{-} brains, Cldn3 was expressed at low levels in brain vessels at P4 and P7 (Fig. S1) and was consistently expressed in all vessels at P14 (Fig. 2 A, a). In Cre^{+} littermates, Cldn3 was strongly reduced in most brain

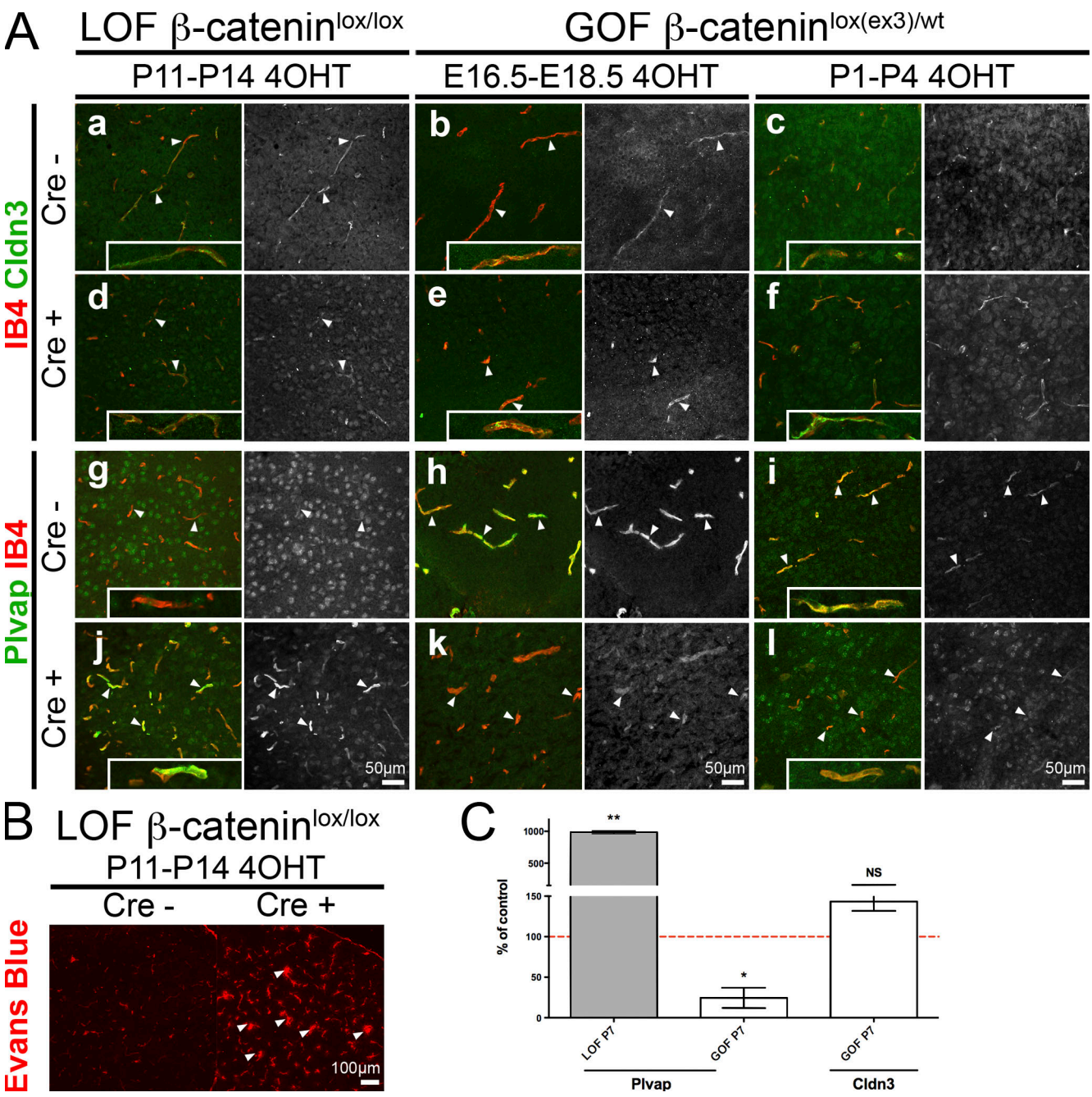

Figure 2. **Conditional β-cat GOF or LOF in ECs in vivo modulates Cldn3 and Plvap expression and permeability in brain capillaries.** P14 brain sections of 4OHT-treated LOF mice stained for Cldn3 or Plvap together with IB4. (A, a and g) Cre$^-$ control mice. Arrowheads point to Cldn3-positive and Plvap-negative vessels, respectively. (d and j) Cre$^+$ LOF resulted in Cldn3 down- and Plvap up-regulation in ~50% of brain capillaries. Arrowheads point to Cldn3-negative and Plvap-positive vessels, respectively. β-Cat GOF in ECs in vivo by 4OHT treatment. E18.5 and P4 brain sections analyzed for Cldn3 or Plvap (green) together with IB4 (red). (b, c, h, and i) Cre$^-$ control mice. Arrowheads point to weak Cldn3-positive vessels at E18.5 and a slightly higher level at P4 or strong Plvap at E18.5 and a slightly weaker level at P4. (e, f, k, and l) Cldn3 increase in Cre$^+$ mice at E18.5 and P4. Plvap was down-regulated. Left panels show merge of IB4 and Cldn3 or Plvap; right panels show Cldn3 or Plvap alone in black and white. Insets show higher magnifications. (B) Evans blue injection i.p. 18 h before tissue harvesting in LOF mice. Arrowheads point to extravasated Evans blue in Cre$^+$ mice at P14. (C) Quantitative RT-PCR for Plvap at P7 in LOF (n = 3; **, P = 0.0001) and GOF (n = 3; *, P = 0.0382). Cldn3 was statistically NS. Control is set to 100% (dashed line). Error bars represent SEM.

vessels at P4 and P7 (Fig. S1) and in approximately half of the vessels at P14 (Fig. 2 A, d). Conversely, Pvlap was poorly expressed in brain vessels of control animals (Fig. 2 A, g; and Fig. S1) but was strongly up-regulated when β-cat was inactivated (Fig. 2 A, j; and Fig. S1). Quantitative RT-PCR analysis of total brain RNA confirmed strong up-regulation of Plvap mRNA (Fig. 2 C). To functionally test barrier properties, we injected Evans blue i.p. 18 h before tissue harvesting. At P14, extravasated Evans blue was apparent around many vessels after endothelial β-cat inactivation but not in controls (Fig. 2 B). This effect was even more pronounced at earlier (P4 and P7) postnatal stages (Fig. S1). Cldn5 was consistently expressed in Cre$^-$ but was

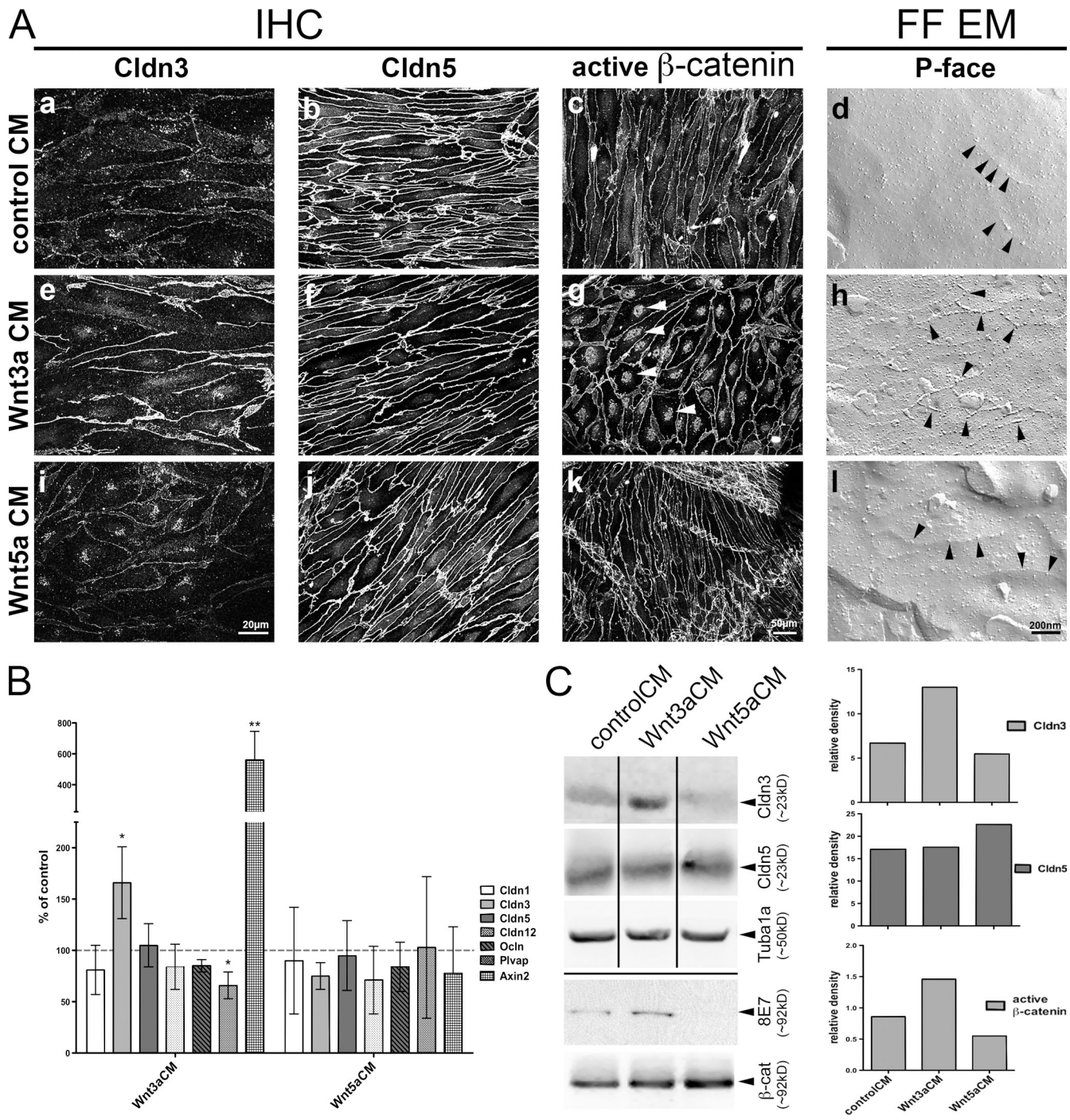

Figure 3. **Wnt3aCM but not Wnt5aCM induced TJs and barrier properties in MBEs.** Wild-type MBEs treated with controlCM, Wnt3aCM, or Wnt5aCM in vitro. (A, a, e, and i) IHC staining for Cldn3. (b, f, and j) IHC staining for Cldn5. Panels are the same magnification as indicated in panel k. (c, g, and k) IHC staining for active β-cat (clone 8E7). Arrowheads point to positive nuclei. (d, h, and l) Freeze-fracture EM. Arrowheads point to P-face–associated TJ ridges. (B) mRNA levels for Cldn1, Cldn3, Cldn5, Cldn12, Ocln, Plvap, and Axin2 measured by quantitative RT-PCR. Cldn3 (n = 3; *, P = 0.0319), Plvap (n = 3; *, P = 0.0098), and Axin2 (n = 3; **, P = 0.005); other tested genes were not significantly altered. Control is set to 100% (dashed line). (C) Western blotting for Cldn3 and Cldn5. α-Tubulin/tubulin α1A served as a loading control. Western blotting for 8E7 and total β-cat. No band could be detected in Wnt5aCM-treated cells. See graphs for densiomeric quantification of bands. Error bars represent SEM. Data are representative of at least three independent experiments.

markedly reduced or absent from most Cre$^+$ vessels at P4 and P7 and strongly reduced in ∼50% of the vessels at P14, suggesting that loss of endothelial β-cat affected the molecular composition of TJs (Fig. S1). Vascular endothelial cadherin (VE-cad) and zonula occludens 1 (ZO-1) were unchanged and localized to all interendothelial junctions (not depicted), whereas plakoglobin (Plako) was slightly increased at adherens junctions of Cre$^+$ samples, confirming previous data showing that Plako can

substitute for the loss of β-cat at adherens junctions in ECs (Fig. S1; Cattelino et al., 2003).

To selectively activate β-cat transcriptional activity in ECs (gain of function [GOF]), we crossed β-cat$^{lox(ex3)/wt}$ mice with Pdgfb-iCreERT2 mice (Harada et al., 1999; Claxton et al., 2008). At E18.5 and P4, Cre$^-$ mice showed only faint Cldn3 staining in brain vessels, whereas Plvap was strongly expressed, confirming the immaturity of the BBB at late embryonic and early postnatal stages (Fig. 2 A, b, c, h, and i). Cre-mediated β-cat activation increased Cldn3 junctional staining at E18.5 and P4 (Fig. 2 A, e and f) and decreased Plvap (Fig. 2 A, k and l). Quantitative RT-PCR confirmed significant down-regulation of Plvap mRNA in Cre$^+$ samples (Fig. 2 C). The Cldn3 mRNA level appeared to be increased, although statistical analysis failed to show significant regulation. The low abundance of this gene in total brain RNA samples is a likely cause for the observed variability and isolation of ECs before RNA extraction may be required to achieve adequate sensitivity in vivo. Nevertheless, even at earlier stages (E13.5), activation of β-cat transcription resulted in detectably stronger junctional Cldn3 staining and reduction of Plvap in brain vessels (Fig. S2, available at http://www.jcb.org/cgi/content/full/jcb.200806024/DC1). Cldn5 expression and localization was not changed between Cre$^+$ and control vessels (Fig. S2). Together, these results illustrate that endothelial β-cat is required for BBB maturation and function in vivo and that transcriptional activation of β-cat accelerates BBB maturation.

Activation of endothelial β-cat signaling induces barrier characteristics in vitro

We next asked whether activation of Wnt/β-cat signaling could reconstitute BBB characteristics in cultured mouse brain microvascular ECs (MBEs). Because it is essentially impossible to culture MBEs from embryos or pups, we developed an in vitro assay using MBEs from young adult mice, which are known to rapidly loose BBB characteristics in culture (Liebner et al., 2000b). Passaged MBEs were cultured for 6 d in either control or conditioned medium (CM) of L cells, producing Wnt3a, which acts through β-cat (Willert et al., 2003), or Wnt5a, which does not stabilize β-cat in ECs (Chen et al., 2003).

Treatment of MBEs with Wnt3aCM resulted in markedly stronger junctional staining of Cldn3 compared with controlCM (Fig. 3 A, a and e). The localization and staining intensity of Cldn5, ZO-1, Plako, and VE-cad was unaffected (Fig. 3 A, b and f; and not depicted). Freeze-fracture analysis revealed more TJ strands in Wnt3aCM-treated cells, regularly showing areas of high protoplasmic fracture face (P-face) association of TJ particles, resembling TJs of BBB ECs in vivo (Fig. 3 A, d and h). As a control, we activated MBEs with Wnt5aCM, which closely corresponds to control conditions concerning Cldn3, Cldn5, and active β-cat staining as well as TJ particle distribution on the P-face (Fig. 3 A, i–l). Quantitative RT-PCR and Western blotting confirmed the up-regulation of Cldn3 in Wnt3aCM but not in Wnt5aCM-stimulated cells on the mRNA and protein level, respectively (Fig. 3, B and C). As expected, nuclear immunolabeling and Western blotting of activated β-cat and induction of the canonical Wnt target gene Axin2 (Fig. 3, A, [c, g, and k], B, and C) were strongest in Wnt3aCM-treated cells, confirming β-cat stabilization by Wnt3aCM. None of these parameters were induced by Wnt5aCM. Other junctional proteins, including Cldn5, VE-cad, β-cat, Plako, ZO-1, Ocln, Cldn1, and Cldn12 were not modified in distribution and expression (Fig. 3 and not depicted).

To directly validate the role of β-cat in Cldn expression, we genetically deleted or stabilized β-cat in ECs in vitro by harvesting brain ECs from β-cat$^{lox/lox}$ and β-cat$^{lox(ex3)/lox(ex3)}$ mice, respectively (Harada et al., 1999; Brault et al., 2001). Cells were treated with cell-permeable transactivating regulatory protein (TAT)–Cre to achieve loxP site–mediated recombination, thus generating β-cat LOF and GOF in vitro (Wadia et al., 2004). β-cat$^{lox/lox}$ cells grew and behaved as wild-type cells, showing Cldn3 up-regulation upon Wnt3aCM treatment (Fig. 4, A [a and b], B, and C), an effect abrogated by the loss of β-cat (Fig. 4, A [c and h] and C).

In contrast, β-cat stabilization led to an increase in Cldn3 junctional staining, mRNA, and protein level (Fig. 4, A [d, e, i, and j], B, and C). A double band for β-cat in the Cre$^+$/β-cat$^{lox(ex3)/lox(ex3)}$ cell extract demonstrates the effective, although not complete, recombination of exon3 by the Cre recombinase. Thus, the effects of β-cat stabilization are comparable with those of stimulating the cells with Wnt3aCM. When we infected a nonbrain-derived endothelioma cell line (Lampugnani et al., 2002) exhibiting low barrier properties with N-terminal truncated β-cat, we observed a significant increase in Cldn3 and barrier properties (freeze-fracture analysis and decrease in Pvlap), suggesting that elevated β-cat transcriptional activity may induce BBB properties also in nonbrain-derived ECs (Fig. S3, available at http://www.jcb.org/cgi/content/full/jcb.200806024/DC1).

Cldn3 up-regulation requires transcriptionally active rather than junctional localized β-cat in MBEs in vitro

To better discriminate the effects of junctional versus transcriptional active β-cat on Cldn3 regulation, we infected MBEs with an adenoviral vector containing dominant-negative TCF4 (dnTCF4; Quasnichka et al., 2006), which inhibits signaling but does not affect the junctional pool of β-cat. Alternatively, MBEs were infected with a lentiviral vector containing LefΔN-βCTA, which dominantly induces β-cat signaling without binding to VE-cad (Vleminckx et al., 1999). Adenoviral infection with dnTCF4 completely abrogated the Wnt3aCM-mediated up-regulation of Cldn3 and Axin2 in primary MBEs, whereas Plvap was significantly up-regulated (Fig. 5, A [a–c] and B [a]).

Lentiviral infection of the dominant-active LefΔN-βCTA construct had principally the same, but a notably stronger, effect than Wnt3aCM, namely Cldn3 up-regulation and Plvap down-regulation (Fig. 5, A [d] and B [b]). Together, these results show that the transcriptional activity of β-cat is necessary and sufficient to up-regulate Cldn3 and down-regulate Plvap, leading to increased barrier properties of brain ECs.

Cldn3 is an important downstream effector of β-cat signaling, whereas Cldn5, although affected in vivo by the loss of β-cat, appears to be ubiquitous and more stably expressed. Although newborn Cldn5-null mice die immediately after birth

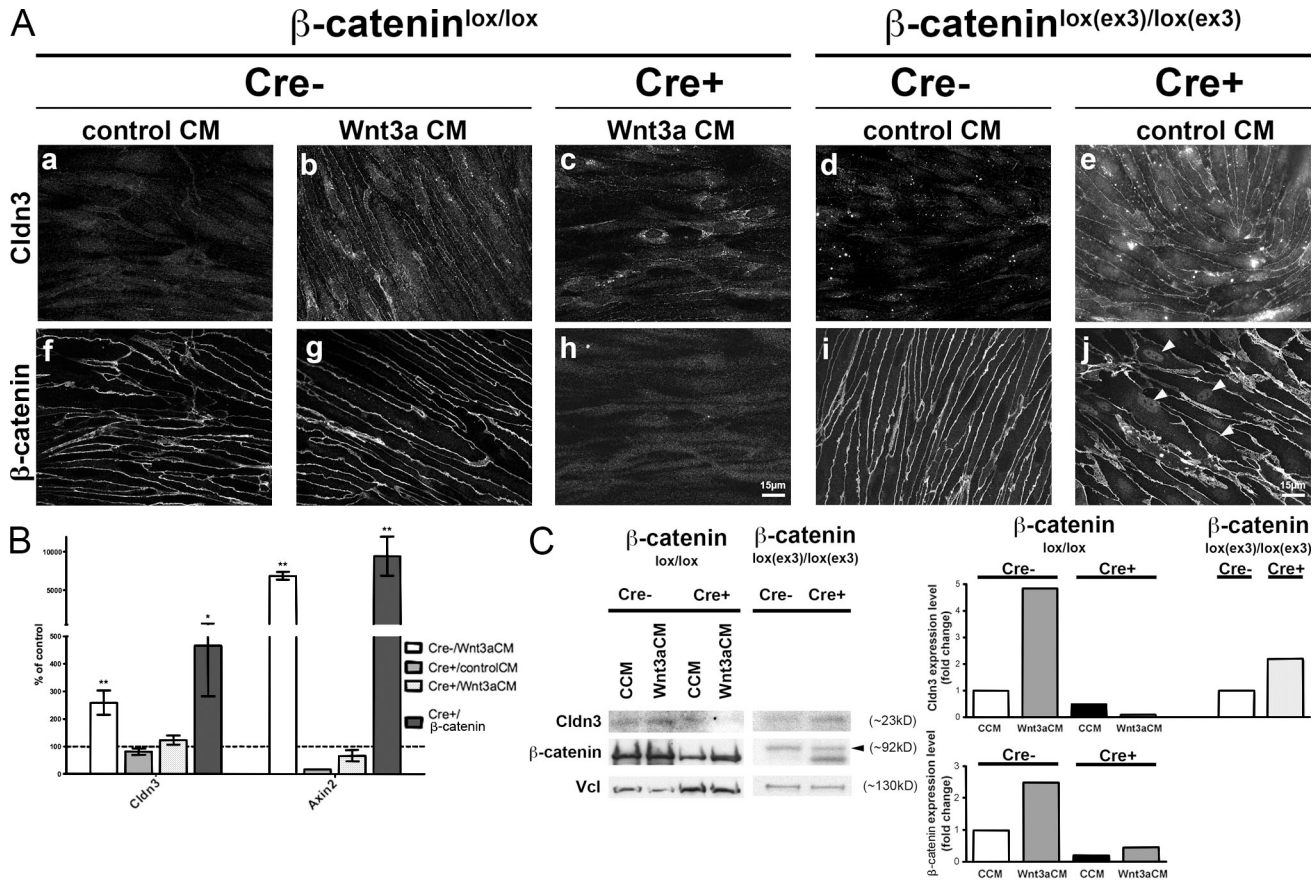

Figure 4. **β-Cat LOF and GOF in MBEs in vitro.** β-Cat$^{lox/lox}$ and β-cat$^{lox(ex3)/lox(ex3)}$ MBEs were treated with TAT-Cre in vitro to achieve β-cat LOF and GOF, respectively. (A, a–c and f–h) β-Cat$^{lox/lox}$ with or without TAT-Cre, stimulated with controlCM (CCM) or Wnt3aCM. IF staining reveals increased junctional Cldn3 in Cre^{-}/Wnt3aCM and a complete absence of β-cat in Cre^{+}/Wnt3aCM. (d, e, i, and j) β-Cat$^{lox(ex3)/lox(ex3)}$ MBEs with or without TAT-Cre, and IF stained for Cldn3 and β-cat. Arrowheads point to nuclear β-cat. (B) Quantitative RT-PCR for Cldn3 in Cre^{-}/Wnt3aCM-treated cells from β-cat$^{lox/lox}$ (n = 3; **, P = 0.0048) and in Cre^{+}/controlCM cells from β-cat$^{lox(ex3)/lox(ex3)}$ (n = 3; *, P = 0.0341) mice. Other tested genes were not significantly altered. Axin2 induction confirmed canonical Wnt signaling in Cre^{-}/Wnt3aCM-treated cells from β-cat$^{lox/lox}$ (n = 3; **, P = 0.0006) and in Cre^{+}/controlCM cells from β-cat$^{lox(ex3)/lox(ex3)}$ (n = 3; **, P = 0.0029) mice. Controls are set as 100% (dashed lines). Error bars represent SEM. (C) Western blot analysis for Cldn3 in β-cat$^{lox/lox}$ and β-cat$^{lox(ex3)/lox(ex3)}$ cells. Transcription and translation of an N-terminal truncated form of β-cat are detected by the anti–β-cat antibody and represented by the bottom band in β-cat$^{lox(ex3)/lox(ex3)}$/Cre^{+} cells. See graphs for densiomeric quantification of Western blot bands. Data are representative of at least three independent experiments.

for defective BBB (Nitta et al., 2003), data reported in this study and in previous work (Wolburg et al., 2003) strongly suggest that Cldn3 is a major determinant of BBB, cooperating with Cldn5 in maintaining low permeability. The precise mechanism through which β-cat regulates the expression of Cldn3 is yet to be defined, but the promoter contains consensus-binding domains for the TCF–Lef–β-cat transcriptional complex (unpublished data). Recently, we demonstrated that β-cat can stabilize FoxO-1 binding to the Cldn5 promoter, contributing to its repression (Taddei et al., 2008). In this study, we found that β-cat in vivo is required to maintain high levels of Cldn5 expression in brain microvasculature. Although we do not know the exact mechanism of this regulation in brain microvasculature, it is likely that the transcriptional role of β-cat varies depending on the specialized region of the vascular tree. Other BBB-related Cldns, such as Cldn1 and Cldn12, were not significantly modified by β-cat signaling.

In this study, we mostly focus on the role of canonical Wnt signaling on vascular junction organization and permeability control. However, other barrier-associated genes may also be controlled by Wnt/β-cat. Recently, the transporters p-glycoprotein and MDR-1 were shown to be up-regulated by specific GSK3β inhibitors in rat brain ECs (Lim et al., 2008). Our own preliminary results did not confirm a regulation of p-glycoprotein and MDR-1 but indicate that Abcg2 and the glucose transporter Slc2a1 were notably up-regulated in MBEs by Wnt3aCM (unpublished data). Although further studies need to elucidate the entire set of BBB-related genes directly or indirectly regulated by Wnt/β-cat, these findings fit well with the concomitant down-regulation of Plvap by active β-cat in vitro and in vivo. Plvap is associated with vessels with high vesicular transport and negatively correlates with the development of the BBB (Hallmann et al., 1995). Conversely, BBB microvessels up-regulate Plvap under pathological conditions such as Alzheimer's disease, brain tumors, and stroke (Sparks et al., 2000; Carson-Walter et al., 2005).

In conclusion, we provide first and direct evidence for the role of the canonical Wnt pathway as a key regulator of the BBB phenotype in ECs. The BBB is indispensable for brain function, and understanding the molecular mechanisms, which determine

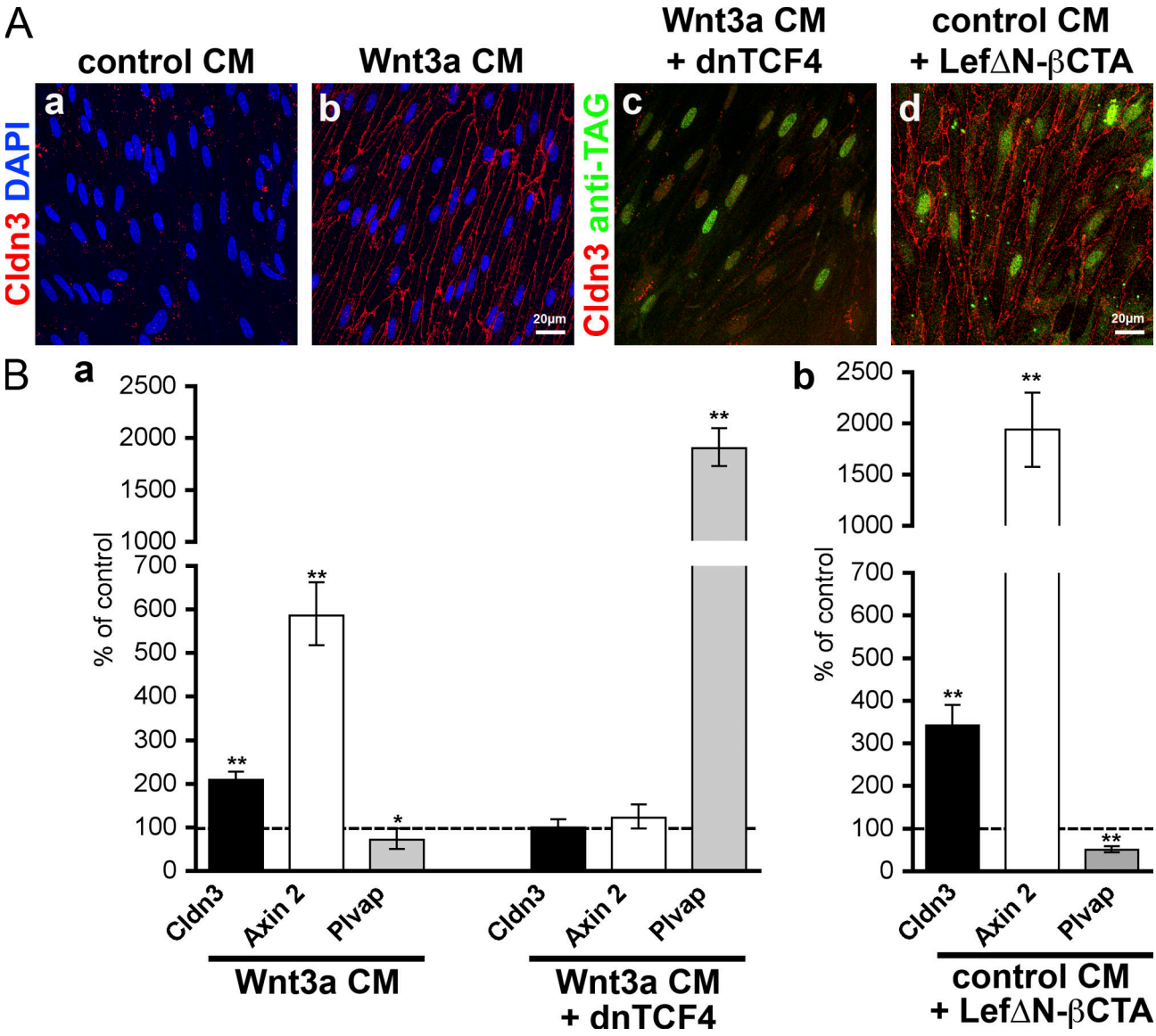

Figure 5. **Cldn3 up-regulation requires transcriptionally active rather than junctional β-cat in MBEs in vitro.** (A, a–c; and B, a) MBEs were either treated with Wnt3aCM or control CM and infected with dnTCF4 adenovirus or a control. (A, a–c) IF stainings for Cldn3. dnTCF4 abrogated the effect of Wnt3aCM on junctional Cldn3. (B, a) Quantitative RT-PCR for Cldn3 (n = 3; **, P = 0.0095), Plvap (n = 3; *, P = 0.035), and Axin2 (n = 3; **, P = 0.004) with Wnt3aCM and for Plvap (n = 3; **, P = 0.002) with Wnt3aCM and dnTCF4. (A, d; and B, b) MBEs infected with LefΔN-βCTA lentivirus or a control. Junctional localization of Cldn3 increased in IF stainings. Quantitative RT-PCR for Cldn3 (n = 3; **, P = 0.002), Plvap (n = 3; **, P = 0.008), and Axin2 (n = 3; **, P < 0.0001). Controls are set as 100% (dashed lines). Green nuclei show an anti–V5-TAG (c) and an anti–HA-TAG (d) staining of dnTCF4 and LefΔN-βCTA, respectively, confirming infection of the target cells. Error bars represent SEM.

barrier properties in ECs, will greatly contribute to the development of new therapeutic strategies to modulate the BBB in the treatment for stroke, multiple sclerosis, and brain tumors.

Materials and methods

Animals

The following transgenic mouse strains were used: β-cat$^{lox(ex3)/lox(ex3)}$ (Harada et al., 1999), β-cat$^{lox/lox}$ (Brault et al., 2001), Pdgfb-iCreER (Claxton et al., 2008), and BAT-Gal/C57Bl6 (Maretto et al., 2003). For MBE preparation, C57Bl6 wild-type mice were used (Charles River Laboratories).

Preparation of primary mouse brain ECs

Mouse brain microvascular fragments were processed as described previously (Liebner et al., 2000b; Calabria et al., 2006). Capillary fragments were seeded in culture medium (DME, 20% FCS, 100 µg/ml heparin, 5 µg/ml EC growth supplement [homemade from calf brain], 100 U/L penicillin/streptomycin, 2 mM glutamin, 1× MEM, and 1 mM Na-pyruvate) at a density of 1.5 × 10^4 cells/ml on collagen I–coated wells. ECs were selected for puromycin (4 µg/ml) resistance for 2 d, grown to confluency and passaged 1:2, and grown for an additional 6 d in the presence of control, Wnt3a, or Wnt5aCM. Cells were fixed with methanol for immunofluorescent staining or lysed for RNA and protein, respectively.

Viral preparations

The lentiviral construct LefΔN-βCTA lacking the armadillo repeats with constitutive TCF–β-cat transcriptional activity was used. The day after splitting, MBEs were infected with lenti-GFP or lenti–LefΔN-βCTA (provided by K. Vleminckx, University of Gent, Gent, Belgium; Vleminckx et al., 1999) and fixed or extracted after 1 wk. Lentiviral and packaging plasmids were provided by L. Naldini (San Raffaele Telethon Institute for Gene Therapy, Milan, Italy) and produced as described previously (Dull et al., 1998). Adenoviral dnTCF4 was provided by S.J. George (Bristol Heart Institute, Bristol, England, UK; Quasnichka et al., 2006). The day after splitting, one

set of cells was treated with Wnt3aCM, and when they reached confluency, they were infected with Ad-GFP or Ad-dnTCF4. 72 h later, the infection cells were fixed or extracted for quantitative RT-PCR.

Conditional deletion/activation of β-cat in vivo and in vitro

ECs were treated with 50 µg/ml TAT-Cre for 60 min in DME without serum followed by 100 µM chloroquine for 30 min (Wadia et al., 2004). The cells were washed with DME and cultured with complete medium with or without WntCM.

For β-cat deletion, in vivo Pdgfb-iCreERT2 (Claxton et al., 2008) lines were crossed to mice harboring floxed alleles of β-cat (β-cat$^{lox/lox}$; Brault et al., 2001) to obtain homozygous floxed β-cat$^{lox/lox}$ pups, of which 50% also carried one Pdgfb-iCreERT2 allele. 4OHT (Sigma-Aldrich) was dissolved in absolute ethanol at 20 mg/ml, diluted to 4 mg/ml in sterile peanut oil, and injected i.p. at 20 µl/g into pups 3 d before tissue harvesting. When harvesting embryonic tissues at E13.5, the mothers were injected with 1 mg 4OHT at E11.5 and 12.5. For control experiments on promoter activity and recombination frequency, see Online supplemental material.

Evans blue permeability

A 1% sterile solution of Evans blue (Sigma-Aldrich) in PBSa was injected i.p. 18–24 h before the animals were harvested. To remove the Evans blue from the vasculature, the mice were perfused with PBSa while under terminal anesthesia. Frozen 12-µm sections of brain and 15-µm sections of skin were dried onto slides for approximately 10 min at 37°C (provided by G. Elia, Cancer Research Institute, London, England, UK). They were fixed in 4°C acetone for 2 min, air dried, dipped in xylene, and mounted in dibutyl polystyrene xylene (Hamer et al., 2002).

Antibodies

The following mouse mAbs were used: anti–α-tubulin and anti-Cldn5 (Invitrogen), anti–β-cat (BD Biosciences), and antiactive β-cat (8E7; Millipore). Rat anti-PECAM/CD31 clone MEC13.3 mAb has been described previously (Vecchi et al., 1994). Rat anti–VE-cad clone BV13 mAb has been described previously (Lampugnani et al., 2002). Rat monoclonal anti–MECA-32/Plvap mAb was provided by R. Hallmann (University of Münster, Münster, Germany; Hallmann et al., 1995).

The following polyclonal antibodies were used: goat anti–β-galactosidase (Abcam), rabbit anti-Cldn3 and rabbit anti–ZO-1 (Invitrogen), rabbit anti–collagen IV (AbD Serotec), biotinylated isolectin B4 (Sigma-Aldrich), and Alexa Fluor direct-conjugated isolectin 568 and 488 (Invitrogen).

The following secondary antibodies were used: appropriated antibodies and streptavidin conjugates Alexa Fluor 350, 488, 555, 568, and 633 were purchased from Invitrogen (the anti–mouse antibodies were highly cross-absorbed against nonspecific mouse proteins). For nuclear stain on brain sections, Hoechst 333258 was diluted to 1 µg/ml in PBS/0.2% Tween 20 and incubated at RT for 5 min. Alternatively, TOTO-3 (1:1,000; Invitrogen) was used.

Immunohistochemistry (IHC)

β-Galactosidase staining of BAT-Gal embryos was performed as previously described (Liebner et al., 2004). Hindbrains were dissected out from PFA-fixed embryos, washed in PBS, and subjected to isolectin. LacZ was either detected as reflection of the 488-nm laser or by antibody staining as indicated. Eyes were fixed in PFA for 5 min on ice, and retinas were subsequently dissected in cold PBSa. Retinas were fixed in 4°C methanol and stored at −20°C. Before staining, the retinas were placed in PBSa to rehydrate. Retinas were incubated in blocking buffer (1% BSA + 0.5% Triton X-100 in PBSa) for 1 h. Immunofluorescent staining with anti–collagen IV, Cldn5, MECA-32/Plvap, VE-cad, ZO-1, and β-cat was performed as previously described (Gerhardt et al., 2003). Appropriate Alexa Fluor–conjugated secondary antibodies were used for detection.

Brains were isolated, placed in Tissue Tek (Sakura Finetek), and slowly frozen in liquid nitrogen vapor. 10–12-µm cryosections were fixed and stained as described previously (Liebner et al., 2000a).

Flat mounted hindbrains were analyzed by fluorescence microscopy using a microscope (80i; Nikon;) with a 20× NA 0.75 or 40× NA 1.4 oil/RT objective equipped with a digital camera (DS-5Mc; Nikon). Measurements were performed by using NIS Elements software (version 3.0; Nikon). Alternatively, images were captured by confocal laser-scanning microscopy using a C1si microscope (Nikon) with a 40× NA 1.4 oil/RT objective or an LCS NT microscope (Leica). Retinas and brain sections were analyzed at RT by confocal laser-scanning microscopy using an upright microscope (LSM 510; Carl Zeiss, Inc.) with 405-, 488-, 543-, and 633-nm laser lines. The lenses used were C Apochromat 10× NA 0.45w, Plan-Neofluar 25× NA 0.80w, and C Apochromat 40× NA 1.2w. Digital zoom factor two or three was used for detail panels. Images and stacks were processed using ImageJ (National Institutes of Health) and Photoshop (CS; Adobe).

RNA preparation and quantitative RT-PCR

Total RNA from cultured cells was prepared with the RNeasy Mini kit (QIAGEN) according to the manufacturer's protocol. RNA was reverse transcribed with the Transcriptor First Strand cDNA Sythesis kit (Roche) using 1 µg of total RNA per 20-µl reaction. For real-time PCR reactions, Absolute Quantitative RT-PCR SYBR Green Fluorescein Mix (Thermo Fisher Scientific) was used as described in the protocol on a DNA Engine Opticon 2 (Bio-Rad Laboratories).

The following primers were used for identification: Cldn1 (sense 5′-GATGTGGATGGCTGTCATTGG-3′, antisense 5′-ACACCTCCCAGAAGGCAGAGG-3′), Cldn3 (sense 5′-CGTACAAGACGAGACGGCCAAG-3′, antisense 5′-CACGTACAACCCAGCTCCCATC-3′), Cldn5 (sense 5′-ATGTCGTGCGTGGTGCAGAGT-3′, antisense 5′-GCGCCGGTCAAGGTAACAAAG-3′), Cldn12 (sense 5′-CAGACAGGCTGCTTGGAGAAAC-3′, antisense 5′-AGGCAATACCACACAGGAAGGA-3′), Ocln (sense 5′-GTGAATGGCAAGCGATCATACC-3′,antisense5′-TGCCTGAAGTCATCCACACTCA-3′), Plvap (sense 5′-GACTACGCGACGTGAGATGGA-3′, antisense 5′-AGGATGATAGCGGCGATGAAG-3′), and Axin2 (sense 5′-GCCGACCTCAAGTGCAAACTC-3′, antisense 5′-GGCTGGTGCAAAGACATAGCC-3′) and, as reference for the house keeping genes, RNA polymerase II (sense 5′-ATGAGCTGGAACGGGAATTTGA-3′, antisense 5′-ACCACTTTGATGGGATGCAGGT-3′) and glucose-6-phosphate dehydrogenase (sense 5′-GGACGACATCCGAAAGCAGAGT-3′, antisense 5′-GAATAGACGGTTGGCCTGCATC-3′). Quantitative RT-PCR conditions were 15 min at 95°C, 40 cycles of 15 s at 94°C, 30 s at 60°C, and 30 s at 72°C. For intron less genes, negative RT controls were performed to exclude the possibility of genomic background.

Western blotting

Western blot analysis was performed according to standard protocols. In brief, confluent cells were washed with ice-cold PBS and scraped in lysis buffer (50 mM Tris and 150 mM NaCl, pH 7.4, containing 1% Triton X-100, 1% Nonidet P-40, 0.5% sodium-deoxycholate, 0.1% sodium-dodecyl-sulfate, 1 mM phenylmethylsulfonyl fluoride, 15 µg/ml leupeptin, 71 µg/ml phenanthrolyne, and 20 U/ml aprotine [Sigma-Aldrich]). The insoluble material was removed by centrifugation at 12,000 rpm for 10 min. Alternatively, cultured cells were lysated by boiling in a modified laemli sample buffer (2% SDS, 20% glycerol, and 125 mM Tris-HCl, pH 6.8). The protein content was measured according to the bicinchoninic acid method (Thermo Fisher Scientific). Total cell lysates were separated by SDS-PAGE under reducing conditions, transfered to a nitrocellulose membrane, and analyzed by immunoblotting with specific antibodies.

Freeze fracturing

Freeze fracturing on glutaraldehyde-fixed ECs was performed as previously described (Liebner et al., 2000b). Negatives were digitized, and images were arranged in Photoshop.

Statistical analysis

Results are presented as mean ± SEM. A two-tailed Student's *t* test was used to analyze the difference between two groups. Values were regarded as significant at $P < 0.05$.

Online supplemental material

Fig. S1 shows that conditional inactivation of β-cat in ECs of postnatal mice led to down-regulation of Cldn3 and Cldn5 and increased permeability in brain capillaries. Fig. S2 shows that conditional activation of β-cat transcriptional activity induced Cldn3 only in brain vessels of early postnatal mice. Fig. S3 shows that activated β-cat can induce Cldn3 and TJ formation in a nonbrain-derived endothelioma cell line. Online supplemental material is available at http://www.jcb.org/cgi/content/full/jcb.200806024/DC1.

The MECA-32/Plvap antibody was provided by R. Hallmann. We thank S. Thom, A. Siepmann, and R. Knittel for excellent technical support. Many thanks to G. Elia (London Research Institute, London, England, UK) for frozen sections and advice on IHC and to L. Davinson for proofreading. We are grateful to S. Watling, C. Thrussell, and C. Darnborough for excellent animal husbandry and assistance with tamoxifen and Evans blue injections as well as tissue harvesting.

This study was supported by the Deutsche Forschungs Gemeinschaft (research group 501 vascular homeostasis, PL 158/7-3 to S. Liebner and

K.H. Plate and ME 820/3-6 to H. von Melchner), the Excellence Cluster Cardio-Pulmonary System (S. Liebner and K.H. Plate), Cancer Research UK (J. Babbage and H. Gerhardt), EMBO Young Investigator Program (H. Gerhardt), Associazione Italiana per la Ricerca sul Cancro, Association for International Cancer Research, the European Community (integrated project contract number LSHG-CT-2004-503573; NoE MAIN 502935; NoE EVGN 503254; EUSTROKE integrated project), Istituto Superiore di Sanita, Italian Ministry of Health, the Ministry of University and Research (fund for the cofinancing of research activities of University protocol 2006058482_002), and Fondation Leducq Transatlantic Network of Excellence (E. Dejana).

Submitted: 3 June 2008
Accepted: 30 September 2008

References

Brault, V., R. Moore, S. Kutsch, M. Ishibashi, D.H. Rowitch, A.P. McMahon, L. Sommer, O. Boussadia, and R. Kemler. 2001. Inactivation of the beta-catenin gene by Wnt1-Cre-mediated deletion results in dramatic brain malformation and failure of craniofacial development. *Development.* 128:1253–1264.

Calabria, A.R., C. Weidenfeller, A.R. Jones, H.E. de Vries, and E.V. Shusta. 2006. Puromycin-purified rat brain microvascular endothelial cell cultures exhibit improved barrier properties in response to glucocorticoid induction. *J. Neurochem.* 97:922–933.

Carson-Walter, E.B., J. Hampton, E. Shue, D.M. Geynisman, P.K. Pillai, R. Sathanoori, S.L. Madden, R.L. Hamilton, and K.A. Walter. 2005. Plasmalemmal vesicle associated protein-1 is a novel marker implicated in brain tumor angiogenesis. *Clin. Cancer Res.* 11:7643–7650.

Cattelino, A., S. Liebner, R. Gallini, A. Zanetti, G. Balconi, A. Corsi, P. Bianco, H. Wolburg, R. Moore, B. Oreda, et al. 2003. The conditional inactivation of the β-catenin gene in endothelial cells causes a defective vascular pattern and increased vascular fragility. *J. Cell Biol.* 162:1111–1122.

Chen, W., D. ten Berge, J. Brown, S. Ahn, L.A. Hu, W.E. Miller, M.G. Caron, L.S. Barak, R. Nusse, and R.J. Lefkowitz. 2003. Dishevelled 2 recruits beta-arrestin 2 to mediate Wnt5A-stimulated endocytosis of Frizzled 4. *Science.* 301:1391–1394.

Claxton, S., V. Kostourou, S. Jadeja, P. Chambon, K. Hodivala-Dilke, and M. Fruttiger. 2008. Efficient, inducible Cre-recombinase activation in vascular endothelium. *Genesis.* 46:74–80.

Dull, T., R. Zufferey, M. Kelly, R.J. Mandel, M. Nguyen, D. Trono, and L. Naldini. 1998. A third-generation lentivirus vector with a conditional packaging system. *J. Virol.* 72:8463–8471.

Engelhardt, B. 2003. Development of the blood-brain barrier. *Cell Tissue Res.* 314:119–129.

Engelhardt, B. 2006. Molecular mechanisms involved in T cell migration across the blood-brain barrier. *J. Neural Transm.* 113:477–485.

Furuse, M., and S. Tsukita. 2006. Claudins in occluding junctions of humans and flies. *Trends Cell Biol.* 16:181–188.

Gerhardt, H., M. Golding, M. Fruttiger, C. Ruhrberg, A. Lundkvist, A. Abramsson, M. Jeltsch, C. Mitchell, K. Alitalo, D. Shima, and C. Betsholtz. 2003. VEGF guides angiogenic sprouting utilizing endothelial tip cell filopodia. *J. Cell Biol.* 161:1163–1177.

Hallmann, R., D.N. Mayer, E.L. Berg, R. Broermann, and E.C. Butcher. 1995. Novel mouse endothelial cell surface marker is suppressed during differentiation of the blood brain barrier. *Dev. Dyn.* 202:325–332.

Hamer, P.W., J.M. McGeachie, M.J. Davies, and M.D. Grounds. 2002. Evans Blue dye as an in vivo marker of myofibre damage: optimising parameters for detecting initial myofibre membrane permeability. *J. Anat.* 200:69–79.

Harada, N., Y. Tamai, T. Ishikawa, B. Sauer, K. Takaku, M. Oshima, and M.M. Taketo. 1999. Intestinal polyposis in mice with a dominant stable mutation of the beta-catenin gene. *EMBO J.* 18:5931–5942.

Kniesel, U., W. Risau, and H. Wolburg. 1996. Development of blood-brain barrier tight junctions in the rat cortex. *Brain Res. Dev. Brain Res.* 96:229–240.

Lampugnani, M.G., A. Zanetti, F. Breviario, G. Balconi, F. Orsenigo, M. Corada, R. Spagnuolo, M. Betson, V. Braga, and E. Dejana. 2002. VE-cadherin regulates endothelial actin activating Rac and increasing membrane association of Tiam. *Mol. Biol. Cell.* 13:1175–1189.

Liebner, S., A. Fischmann, G. Rascher, F. Duffner, E.H. Grote, H. Kalbacher, and H. Wolburg. 2000a. Claudin-1 and claudin-5 expression and tight junction morphology are altered in blood vessels of human glioblastoma multiforme. *Acta Neuropathol.* 100:323–331.

Liebner, S., U. Kniesel, H. Kalbacher, and H. Wolburg. 2000b. Correlation of tight junction morphology with the expression of tight junction proteins in blood-brain barrier endothelial cells. *Eur. J. Cell Biol.* 79:707–717.

Liebner, S., A. Cattelino, R. Gallini, N. Rudini, M. Iurlaro, S. Piccolo, and E. Dejana. 2004. β-Catenin is required for endothelial-mesenchymal transformation during heart cushion development in the mouse. *J. Cell Biol.* 166:359–367.

Lim, J.C., K.D. Kania, H. Wijesuriya, S. Chawla, J.K. Sethi, L. Pulaski, I.A. Romero, P.O. Couraud, B.B. Weksler, S.B. Hladky, and M.A. Barrand. 2008. Activation of beta-catenin signalling by GSK-3 inhibition increases p-glycoprotein expression in brain endothelial cells. *J. Neurochem.* 106:1855–1865.

Maretto, S., M. Cordenonsi, S. Dupont, P. Braghetta, V. Broccoli, A.B. Hassan, D. Volpin, G.M. Bressan, and S. Piccolo. 2003. Mapping Wnt/beta-catenin signaling during mouse development and in colorectal tumors. *Proc. Natl. Acad. Sci. USA.* 100:3299–3304.

Moon, R.T. 2005. Wnt/beta-catenin pathway. *Sci. STKE.* doi:10.1126/stke.2712005cm1.

Nitta, T., M. Hata, S. Gotoh, Y. Seo, H. Sasaki, N. Hashimoto, M. Furuse, and S. Tsukita. 2003. Size-selective loosening of the blood-brain barrier in claudin-5–deficient mice. *J. Cell Biol.* 161:653–660.

Quasnichka, H., S.C. Slater, C.A. Beeching, M. Boehm, G.B. Sala-Newby, and S.J. George. 2006. Regulation of smooth muscle cell proliferation by beta-catenin/T-cell factor signaling involves modulation of cyclin D1 and p21 expression. *Circ. Res.* 99:1329–1337.

Sparks, D.L., Y.M. Kuo, A. Roher, T. Martin, and R.J. Lukas. 2000. Alterations of Alzheimer's disease in the cholesterol-fed rabbit, including vascular inflammation. Preliminary observations. *Ann. NY Acad. Sci.* 903:335–344.

Srinivas, S., T. Watanabe, C.S. Lin, C.M. William, Y. Tanabe, T.M. Jessell, and F. Costantini. 2001. Cre reporter strains produced by targeted insertion of EYFP and ECFP into the ROSA26 locus. *BMC Dev. Biol.* 1:4.

Taddei, A., C. Giampietro, A. Conti, F. Orsenigo, F. Breviario, V. Pirazzoli, M. Potente, C. Daly, S. Dimmeler, and E. Dejana. 2008. Endothelial adherens junctions control tight junctions by VE-cadherin-mediated upregulation of claudin-5. *Nat. Cell Biol.* 10:923–934.

Vecchi, A., C. Garlanda, M.G. Lampugnani, M. Resnati, C. Matteucci, A. Stoppacciaro, H. Schnurch, W. Risau, L. Ruco, A. Mantovani, et al. 1994. Monoclonal antibodies specific for endothelial cells of mouse blood vessels. Their application in the identification of adult and embryonic endothelium. *Eur. J. Cell Biol.* 63:247–254.

Vleminckx, K., R. Kemler, and A. Hecht. 1999. The C-terminal transactivation domain of beta-catenin is necessary and sufficient for signaling by the LEF-1/beta-catenin complex in *Xenopus laevis*. *Mech. Dev.* 81:65–74.

Wadia, J.S., R.V. Stan, and S.F. Dowdy. 2004. Transducible TAT-HA fusogenic peptide enhances escape of TAT-fusion proteins after lipid raft macropinocytosis. *Nat. Med.* 10:310–315.

Willert, K., J.D. Brown, E. Danenberg, A.W. Duncan, I.L. Weissman, T. Reya, J.R. Yates, and R. Nusse. 2003. Wnt proteins are lipid-modified and can act as stem cell growth factors. *Nature.* 423:448–452.

Wolburg, H., K. Wolburg-Buchholz, J. Kraus, G. Rascher-Eggstein, S. Liebner, S. Hamm, F. Duffner, E.H. Grote, W. Risau, and B. Engelhardt. 2003. Localization of claudin-3 in tight junctions of the blood-brain barrier is selectively lost during experimental autoimmune encephalomyelitis and human glioblastoma multiforme. *Acta Neuropathol.* 105:586–592.